Quantifying hydrothermal alteration with normative minerals and other chemical tools at the Beattie Syenite, Abitibi greenstone belt, Canada

Lucie Mathieu [1*]

[1]*CONSOREM (CONSOrtium de Recherche en Exploration Minérale - Mineral exploration research consortium), 555 Boulevard de l'Université, Saguenay, Canada, G7H 2B1.*

**Corresponding author (e-mail: mathiel@tcd.ie)*

Abbreviated title: Quantifying alteration at Beattie

Keywords: hydrothermal alteration, mass-balance, alteration indices, alkali metasomatism, Beattie Syenite, Abitibi greenstone belt

Abstract: Methods to quantify hydrothermal alteration are used to: document alteration halos; to comprehend hydrothermal processes; and to prospect for mineralisation formed by such processes. The chemical methods available are numerous and each has specific advantages, limitations and fields of application. This study focuses on the hydrothermal process at Beattie, a Neoarchean gold deposit hosted by the Beattie Syenite within the Abitibi Greenstone Belt, Superior Province, Canada. To quantify alteration, it was necessary to use the following chemical methods: 1) mass-balance calculations; 2) normative minerals and related alteration indices; and 3) Pearce Element Ratios (PER) diagrams. In the study area, silicification and carbonatisation are satisfactorily quantified by alteration indices, while alkali metasomatism was best estimated by mass-balance calculations and PER diagrams. Combining these methods, the following alteration types have been documented: K-feldspar alteration, silicification, and Na-Ca-leaching are intense and proximal to gold mineralisation; carbonatisation is widespread and intense; and sericitisation and chloritisation are minor to absent. It is proposed that, at the Beattie Syenite, the formation of white mica and chlorite and the mobilisation of alkali and silica are consequences of the predominant process related to carbonatisation.

Introduction

Insights into hydrothermal processes can be gained by documenting, for example, the mineral phases gained and lost during the operation of such processes, and by quantifying the mass changes in major elements. Alteration can be estimated from mineralogical and chemical data using numerous methods that each has its specific advantages and disadvantages. Selecting the most pertinent method in a given context is not always straightforward, as will be demonstrated in this contribution using the example of the Beattie Syenite.

Mineral counts and textural observations made in thin sections, for example, are powerful methods that provide a direct insight into alteration processes. Such methods, however, are generally used in an academic context whereas, in an exploration context, less time-consuming methods need to be employed that are nevertheless sufficiently reliable to assist in the discovery and delimitation of orebodies by enabling the recognition, qualification, and quantification of alteration. Mass-balance calculations are useful to exploration and academic proposes and have been used successfully in a variety of contexts (e.g. Barrett & MacLean 1994). Such methods, however, require the sampling of a precursor (i.e. unaltered rock) and the reliable analysis of trace elements (e.g. the isocon method; Grant 1986), which are not always available. Alteration indices calculated from major elements (e.g. Saeki & Date 1980; Kishida & Kerrich 1987) or normative minerals (Piché & Jébrak 2004; Trépanier *et al.* 2015; Mathieu *et al.* 2015) are other commonly used tools. Also, most methods quantify either alteration (mineralogical changes) or metasomatism (chemical changes; Stanley & Madeisky 1994), and produce results that are not equivalent.

Additionally, chemical methods have generally been designed for particular types of alteration. For example, white micas observed in thin sections may have formed as a consequence of: 1) feldspar destruction, Na-Ca-leaching, hydration, and K-gains (sericitisation), which are best quantified by mass-balance calculations (e.g. Grant 1986); or of 2) carbonatisation, which is more reliably estimated by alteration indices calculated by the NORMAT or CONSONORM_LG methods (Piché & Jébrak 2004; Trépanier *et al.* 2015). Also, if the precursor (i.e. fresh rock) is a K-feldspar-barren rock, K-feldspar alteration (as defined by Large *et al.* 2001) can be quantified using the amount of normative K-feldspar or observed microcline, adularia, or orthoclase. With K-feldspar-enriched precursors, however, mass-balance calculations are more reliable.

In this contribution, alteration types recorded by the Beattie Syenite intrusion are documented using a variety of chemical methods. The Beattie Syenite, which hosts the Beattie gold deposit, is a Neoarchean alkaline intrusion within the Abitibi greenstone belt. This lithologically and structurally controlled deposit (Bigot & Jébrak 2015) is associated with silicification, sericitisation, carbonatisation, and K-feldspar alteration (Bigot 2012; Bourdeau 2013). The available chemical data from Bourdeau (2013) are typical of datasets used by exploration geologists and thus, the Beattie Syenite will be used to compare chemical methods that can be realistically used in an exploration context, and to discuss their advantages and limitations. Also, the alteration processes at the Beattie Syenite will be presented and discussed.

Geological setting

The Beattie Syenite, located in Québec, Canada, is part of the Abitibi greenstone belt, a Subprovince of the Superior Province, an Archean craton. The intrusion is located immediately north of the Porcupine-Destor fault zone, which borders the northern part of the Archean composite volcano represented by the Blake River Group (Pearson & Daigneault 2009; McNicoll *et al.* 2014) (Fig. 1). It intrudes meta-sedimentary rocks of

the Porcupine Group and meta-volcanic rocks of the Deguisier Formation (see regional geology in Legault *et al.* 2006, and local mapping by Bourdeau, 2013).

The syenite consists of a main intrusion, which is 3.7 km long and 4 to 70 m thick (surface area of 1.2 km^2), and several minor dykes located within 1 km of the main intrusive body (Bourdeau 2013). The magma was emplaced at ~2682 Ma (David *et al.* 2007; Mueller *et al.* 1996). Gold mineralisation was emplaced before the area was deformed and metamorphosed by low grade regional metamorphism (greenschist facies; 250^{o}C, 220 MPa; Powell *et al.* 1995) between 2677 and 2643 Ma (Legault *et al.* 2006). Gold was mined from the intrusion (25% of the ore) and nearby rocks (75%) from the Beattie, Donchester, and Central Duparquet mines between 1933 and 1956, for a total inferred resource of 2.77 million ounces contained in 56.2 Mt @ 1.53 g/t gold (estimate by Osisko Mining Corporation and Clifton Star Resources Ltd., as cited by Bigot 2012). The petrology of the Beattie Syenite indicates it is homogeneous and dominated by albite and orthoclase. Minor phases include carbonate, white mica, and Fe-Ti oxides (Bourdeau 2013). The main mafic phase prior to carbonatisation may have been clinopyroxene, by analogy with the nearby unaltered Murdock Creek intrusion (see studies by Rowins *et al.* 1991, 1993). Using essentially textural criteria, Bourdeau (2013) distinguished the following lithological units: 1) porphyritic Beattie syenite; 2) equigranular magnetite-bearing syenite; 3) porphyritic Central Duparquet syenite; 4) megaporphyric syenite; and 5) lath syenite.

Chemically, the Beattie Syenite is enriched in Al, with an aluminium saturation index (ASI; Shand 1927) of 0.9 to 1.1 and a peralkaline index (Shand 1951) of ~0.8 (Bourdeau 2013). It is enriched in light rare earth elements (LREE) and large-ion lithophile elements (LILE), shows fractionated REE (La/Yb ~40), and displays a Ti-Nb-Ta negative anomaly on a spider-diagram (Pearce 2008; Fig. 2), as do the other alkaline intrusions observed in Abitibi (see intrusions studied by Beakhouse 2011; Bourne & l'Heureux 1991; Dejou 1992; Martin 2012; Rowins *et al.* 1993).

The main alteration types related to the Beattie gold deposit and observed in the intrusive rocks are: 1) carbonatisation, which formed calcite and iron-enriched carbonates (Boudreau 2013; Legault & Lalonde 2009); 2) sericitisation, which formed ferriferous white mica (Bigot & Jébrak 2015; Bourdeau 2013); and 3) K-feldspar alteration, which formed K-feldspar (Davidson & Banfield 1944; Legault & Lalonde 2009). Late alteration also formed gold-bearing carbonate-albite-quartz-veins (Bourdeau 2013).

The compositions of the intrusive rocks of the Beattie Syenite are documented by 185 chemical analyses compiled by Bourdeau (2013) from various sources (Table 1). These chemical analyses were obtained from samples collected during surface mapping, exploration, and exploitation, and mostly document the porphyritic Beattie syenite unit. The scarcity and variable quality of Zr, Cr, Y, Th, and Nb analyses (Table 1) prevents the modelling of precursor compositions with Trépanier's method (Trépanier *et al.* 2016). For the requirements of this study, a precursor was selected that corresponds to the average composition of five least-altered samples published by Bigot & Jébrak (2015)

(Table 2). In the following sections, various methods will be used to quantify alteration using these chemical data.

Method 1: mass-balance calculations

Mass-balance calculations are powerful methods that have two main requirements: 1) recognition of a fresh or least-altered sample (precursor); and 2) reliable Al_2O_3, TiO_2, and, if available, trace-element analyses. Mass-change methods, which are numerous (Grant 1986; MacLean & Barrett 1993; Barrett & MacLean 1994), are based upon the equation of mass transfer (Equation 1) (Gresens 1967; Leitch & Lentz 1994). At Beattie, Bourdeau (2013) used the Isocon method (Grant 1986, 2005) to conclude that Au enrichments correlate with increases in CO_2, K, Si, As, S, Ag, W, Sb, Hg, Bi, W, Cu, and Mo, and decrease in Na, Sr, Ba, Ga, Sn, and Pb. Here, the procedure of Barrett & MacLean (1994), which is a direct application of Equation 1, is used. Calculations are performed on analyses recalculated to 100% anhydrous with iron as FeO^T.

$$X_n = W^B - W^A = (X^A_{immobile} / X^B_{immobile})(X^B_n) - X^A_n \quad (1)$$

where:

- X_n = mass change of chemical element "n"
- W^B, W^A = weight of element "n" in precursor (A) and in altered rock (B)
- $X^A_{immobile}$, $X^B_{immobile}$, X^A_n, X^B_n = proportions (wt% or ppm) of an immobile element, and of element "n", in the precursor (A) and in the altered (B) rock.

Potential immobile elements are Al_2O_3 and TiO_2, as well as several trace elements (Cr, Nb, Th, Y, and Zr). However, trace elements analyses are only available for a limited number of samples (Table 1) and will not be used to perform mass-balance calculations.

The Beattie Syenite is a felsic intrusion with a homogeneous petrology (Bourdeau 2013) that might have been chemically homogeneous prior to alteration (i.e. single precursor). In a single precursor system, a linear alteration trend should be observed on an Al_2O_3 and TiO_2 binary diagram (Fig. 3), which should pass through the precursor and the origin of the diagram (Barrett & MacLean 1994). Two main alteration trends (Groups I and II) and isolated samples (Group III) are however observed on an Al_2O_3 vs TiO_2 graphic (Fig. 3). Note that the groups identified in Fig. 3 do not correlate with the lithological units identified by Bourdeau (2013).

To illustrate pre-alteration range in chemical composition, the Murdock Creek pluton is compared to the Beattie Syenite. Murdock Creek is an alkaline intrusion of Abitibi that has not been altered (Rowins *et al.* 1991, 1993) and, on the Al_2O_3 and TiO_2 binary diagram, rocks differentiated by fractional crystallisation align along a fractionation trend (Fig. 3-a). A similar fractionation trend likely existed at the Beattie Syenite prior alteration (Fig. 3-b). Group I samples likely belong to the dominant felsic unit, while Group III samples may belong to a more differentiated unit (multiple precursor system; Barrett & MacLean 1994). Similarly, a more mafic precursor may be proposed for Group II samples. Major differences between Groups I and II precursors are, however, not

supported by petrological observations (Bourdeau 2013). Alternatively, Group II samples may contain clusters of Ti-bearing minerals, such as titanite and white mica, which locally re-distributed Al and Ti and modified the Al/Ti ratios of the rocks. Mass balance will not be calculated on these samples.

The samples representing the available precursor (from Bigot & Jébrak 2015) are all assigned to Group I (Fig. 3-b). Mass-change calculations are performed on these rocks only and using Al_2O_3 as the conserved element (Fig. 4, 5). Group I contains 141 samples with a correlation coefficient of Al_2O_3 and TiO_2 of 0.75. The most distinctive mass-changes correspond to K_2O and SiO_2 gains, and Na_2O losses (Fig. 4). Only 13 rocks gained > 1% Na_2O (Fig. 5). Most SiO_2 mass changes are within -1.86% (Q1, 25th percentile) and 11% (Q3, 75th percentile), except for 5 samples with mass changes > 100%. These 5 samples likely contain quartz-veins. Na_2O and K_2O mass changes are anti-correlated, except for two strongly silicified samples that may contain quartz-veins (Fig. 5). Most silica and alkali mass changes are within 5%, except for 36 samples that lost > 4% Na_2O and gained > 6% K_2O and > 5% SiO_2 (Fig. 5). The rocks also lost CaO and minor amounts of FeO and MgO (Fig. 4).

Method 2: alteration minerals

In this section, alteration indices are calculated using mineral proportion ratios. As mineralogical observations are not available for all samples, normative minerals and indices (Table 3) are calculated with CONSONORM_LG, a method designed for mining exploration datasets (Trépanier *et al.* 2015). The CONSONORM_LG norm is calculated for the 2SV350 model (standing for 2 kbars, 350^{O}C, with "SV" referring to greenschist facies) and using a Fe_2O_3/Fe_2O_{3TOT} ratio of 0.4 (following Middlemost 1989). CO_2 is analysed for 80 samples and, for the remaining rocks, CO_2 was estimated from the LOI and the norm (see Trépanier *et al.* 2015 for details). Results of this calculation are summarised in Table 4 and Fig. 6.

Normative minerals consist essentially of orthoclase (19-41 vol%), albite (8-46 vol%), quartz (7-22 vol%), muscovite (3-12 vol%), carbonates (3-11 vol%), oxide Fe-Ti (1-2 vol%, magnetite mostly), and chlorite (< 3 vol%). By comparison, minerals observed in thin sections comprise the following: 35-45 vol% albite, 35-40 vol% orthoclase, 5-10 vol% carbonate, 0-15 vol% white micas, 0-5 vol% hematite and, for the equigranular syenite unit only, 7 vol% actinolite and 10 vol% magnetite (Bourdeau 2013). Accessory minerals (< 1 vol%) are also observed: apatite, titanite, biotite, chlorite, fluorite, xenotime, tourmaline, hornblende, epidote, barite, sulphides, and quartz (Banfield 1940; Bourdeau 2013; Bigot & Jébrak 2015). There is no discrepancy between observed and calculated minerals except for quartz, which is rarely reported from thin-section observations (Bourdeau 2013).

According to the normative calculation, the proportions of the most abundant phases, and especially those of the alkali feldspars, are highly variable amongst samples (Fig. 6-a). Also, compared to the normative composition of the precursor, most rocks contain less albite, more white mica, quartz, and carbonate, and variable amounts of orthoclase (Fig.

6-a). Because the precursor contains little to no white mica, quartz, or carbonate, the alteration indices reported in Table 4 can be used to estimate the intensity of sericitisation, silicification, and carbonatisation. These indices, which can take values between 0 and 100, indicate that sericitisation and chloritisation are negligible (ALT_MUSCV, ALT_CHLO), silicification is moderate to locally intense (ALT_QTZ), and that carbonatisation is generally intense (ALT_SER_CARBS, ALT_CARBS) (Table 4, Fig. 6-b).

The main sericitisation reactions involve K_2O gain (Equation 2; Barrett & MacLean 1994) or carbonatisation (Kishida & Kerrich 1987). By comparison with the Murdock Creek pluton, the pre-alteration rocks of the Beattie Syenite were likely dominated by alkali feldspar and clinopyroxene, and carbonatisation of these rocks may have formed quartz, carbonate, muscovite, and chlorite, and leached Na, K, Fe, and Mg (Equation 3). Note that this carbonatisation reaction should be tested by dedicated petrological studies. The ALT_SER_CARBS index reaches values much larger than those attained by the ALT_MUSCV and ALT_CHLO indices, indicating that most white mica and chlorite likely formed as a consequence of carbonatisation (Equation 3).

$$\underset{\text{albite}}{3\ NaAlSi_3O_8} + \underset{\text{fluid}}{K^+ + 2\ H^+} \leftrightarrow \underset{\text{muscovite}}{KAl_3Si_3O_{10}(OH)_2} + \underset{\text{quartz}}{6\ SiO_2} + \underset{\text{fluid}}{3\ Na^+} \quad (2)$$

$$\underset{\text{clinopyroxene}}{5\ (Fe,Mg)CaSi_2O_6} + \underset{\text{alkali feldspar}}{20\ (Na,K)AlSi_3O_8} + \underset{\text{fluid}}{5\ CO_2 + 17.8\ H^+} \leftrightarrow \underset{\text{quartz}}{49.3\ SiO_2} + \underset{\text{calcite}}{5\ CaCO_3} \quad (3)$$

$$\underset{\text{clinochlore}}{0.6\ (Mg,Fe)_5Al_2Si_3O_{10}(OH)_8} + \underset{\text{muscovite}}{6.25\ KAl_3Si_3O_{10}(OH)_2} + \underset{\text{fluid}}{13.8\ (Na+K)^+ + 2\ (Fe+Mg)^{2+} + 0.5\ H_2O}$$

Alkali metasomatism is estimated using the normative proportions of albite and K-feldspars; i.e. indices ALT_ALB and ALT_KFS (Table 4). However, in order for alteration to be quantified meaningfully, alteration indices should be equal to 0 in precursors, which is not the case for the ALT_ALB and ALT_KFS indices because the Beattie Syenite contained abundant alkali feldspars prior to alteration. As such, interpreting the values of these indices would require comparison with normative composition of the precursor, and alteration indices are not adapted to such situations. An alternative method is used hereafter to quantify K-feldspar alteration.

Method 3: PER diagrams

Quantifying alteration can also be achieved using Pearce Element Ratio (PER) diagrams (Pearce 1968) adapted for hydrothermal alteration processes (Stanley & Madeisky 1994). The PER diagrams designed for feldspars are here used to investigate Na and K compositional variations and to quantify alteration-related deviations from the orthoclase/albite ratio of the precursor.

The PER diagram method requires the identification of a conserved element that is immobile in the hydrothermal fluid and incompatible in the fractionating minerals.

Immobile elements available for the bulk of samples are Al and Ti, with Al being a major constituent of feldspar. The conserved element considered here is Ti.

On the PER diagrams for feldspar (Fig. 7-a, b), most samples do not significantly depart from a line with a slope of 1 (Stanley & Madeisky 1994), indicating that feldspar fractionation may explain compositional variations of Al, Na, K, and part of Ca. On the PER diagram for alkali feldspar (Fig. 7-c), the regression line has a slope of 0.75, indicating that most of the Al variability can be explained by alkali feldspar fractionation. Samples departing from the regression lines, on the PER diagrams for feldspars (Fig. 7-a, b, c), likely contain additional Al-bearing mineral phases such as the alteration minerals white mica and chlorite.

On the (Na+K)/Ti vs Al/Ti (molar) diagram (Fig. 7-c), only a minority of samples plot near a regression line with a slope of 1/3 and have likely been intensely sericitised. On the K/Ti vs Al/Ti (molar) diagram (Fig. 7-d), samples are not aligned because the K/Na ratio of alkali feldspar is variable amongst samples (Fig. 6-a). Rocks of Group I have similar Al/Ti ratios and degrees of differentiation (Fig. 3-b). Prior to alteration, these rocks likely had orthoclase/albite and K/Na ratios similar to these of the samples representing the available precursor (from Bigot & Jébrak 2015). This precursor has a K/Na (molar) ratio of 0.3/0.55.

On the K/Ti vs Al/Ti (molar) diagram (Fig. 7-d), the samples located near a line going through the origin and the samples representing the precursor have retained the K/Na ratio of their precursors and likely gained and lost negligible amounts of alkali. On this diagram, maximal K-feldspar alteration and albitisation are attained by samples aligned along the y=x and y=0 lines, respectively.

The K/Na (molar) ratios of altered samples are compared to that of the precursor (0.3/0.55) using the PER_K index, which quantifies relative K_2O mass changes (Equation 4). The PER_K index ranges between 100 (maximal K-gain) and -100 (maximal K-loss or Na-gain) and if the result is < -100, then a value of -100 is assigned to the index.

$$\text{PER\_K index} = 100\times[1 - (0.3/0.55)/(K/Na)] \text{ (molar)} \quad (4)$$

The PER_K index is calculated for the 141 samples of Group I. Calculation of this index is not extended to Groups II and III samples because constraints on the K/Na (molar) ratios of the precursors to these rocks are not available. For Group I samples, the PER_K index has mean, median, Q1, and Q3 values of 33.46, 45.90, -0.30, and 89.43, respectively. Most values are positive, indicating that K-gains dominate.

Spatial distribution of alteration types

In this section, the spatial distribution and relation with gold grades of alteration types are presented. Potassium metasomatism is documented by bulk of the chemical methods, and the values of the PER_K index and K_2O mass changes are comparable (Fig. 8-a). Using the PER_K index, K-gains are mostly located in the western and eastern extremities of

the Beattie Syenite (Fig. 9-a). Carbonatisation is documented by the ALT_CARBS index and is most intense in the central part and western extremity of the intrusion (Fig. 9-b). Silicification is documented by the ALT_QTZ index and SiO_2 mass changes and both methods produce consistent results (Fig. 8-b). Silicification is mostly observed in the western extremity of the intrusion (Fig. 9-c). A spatial correlation was noted between CaO and Na_2O mass changes, which have been summed and displayed in map view (Fig. 9-d). Leaching of these elements is most intense in the eastern and western extremities of the intrusion (Fig. 9-d).

Alteration intensity has then been correlated to mineralisation using the Au analyses that are available for 151 samples (Table 5). Gold values correlate positively with: 1) Si-gains, based on SiO_2 mass changes and the ALT_QTZ index; and 2) K-gains, based on K_2O mass changes and the PER_K index. Gold values and Na_2O mass changes are also negatively correlated (Table 5). Elevated gold values are mostly located in the western extremity of the intrusion (Beattie mine area), where K-feldspar alteration, silicification, and Ca-Na-leaching are the most intense (Fig. 9). In the eastern part of the intrusion (Central Duparquet mine area), only K-feldspar alteration and Ca-Na-leaching are intense (Fig. 9-a, d). Carbonatisation, on the other hand, does not correlate with gold values, is observed in the whole intrusion and is particularly intense in the central part of the Beattie Syenite (Fig. 9-b).

Discussion

Dominant alteration types at the Beattie Syenite are K-feldspar alteration, Ca-Na-leaching, carbonatisation, and silicification. The intensity and possible processes of these alteration types are discussed, prior to focusing the discussion on the performance of the methods.

Alteration intensity

Alkali compositional variations are documented by the proportions of normative albite, K-feldspars and related indices, the PER_K index, and mass-balance calculations. These methods indicate that K_2O and Na_2O mass changes are anti-correlated and that K_2O gains dominate. Sericitisation is minor according to the ALT_MUSCV index, and most K_2O gains are likely related to K-feldspar alteration.

The PER_K index can vary between -100 and 100. Values > 50 for this index, which correlate with K_2O mass changes > 2% (Fig. 8-a), could be considered as intermediate to intense K-feldspar alteration (Table 6). As such, 56 samples (out of 141) display intense K-feldspar alteration, and these samples are also characterised by: 1) ALT_KFS index > 38; 2) ALT_ALB index < 42; 3) normative orthoclase > 20 wt%; 4) normative albite < 40 wt%; and 5) Na_2O mass changes < -1.42%.

Carbonatisation is documented by the CONSONORM_LG method only. The ALT_CARBS index has mean, median, Q1, and Q3 values of 66.90, 72.81, 51.48, and 93.99, respectively (Fig. 6-b). As this index can vary between 0 and 100, carbonatisation

is interpreted to be generally intense (Table 6). The median values for the normative proportion of carbonates (mostly calcite) and for the amount of CO_2 wt% calculated by the CONSONORM_LG method are 5.90 wt% and 2.63 wt%, respectively. The amount of Ca, Fe, and Mg available to form carbonates is limited at Beattie, where carbonatisation is intense even if only a small amount of CO_2 wt% has been introduced to the system.

Silicification is documented by the ALT_QTZ index and SiO_2 mass changes. Most samples (140 out of 185) have index values < 25 and contain < 22 wt% of normative quartz. Also, 127 samples (out of 141) have ALT_QTZ index values and SiO_2 mass changes < 25 and 25%, respectively. The ALT_QTZ index can vary between 0 and 100, and a value of 25 could be considered low and may characterise weakly silicified samples. However, for rocks that likely contained < 5 wt% quartz prior to alteration (see composition of the precursor; Table 4), an increase in the normative proportion of quartz of about 10-20 wt% may correspond to relatively intense silicification (Table 6). Silicification is thus interpreted to be generally intermediate to intense.

The other alteration types documented include CaO losses, which correlate with Na-leaching. It has been proposed that K_2O mass changes > 2% correspond to significant K-gains: by analogy, Na_2O + CaO mass changes < -2% are interpreted as intense Ca-Na-leaching (Table 6).

Chloritisation and Fe-Mg-losses are also quantified by mass-balance calculations and the ALT_CHLO index. The Beattie Syenite likely contained minor proportions of mafic minerals prior to alteration. For such rocks, it is proposed that chloritisation be considered significant for FeO and MgO mass changes of ± 1% and ALT_CHLO index > 25 (Table 6). Using such thresholds, it is concluded that chloritisation is negligible.

Using the threshold values proposed here and summarised in Table 6, the main alteration types are displayed in map view (Fig. 10). The area located at the western extremity of the intrusion and immediately south of the orebody exploited by the Beattie mine is characterised by intense carbonatisation, K-feldspar alteration, silicification, and Na-Ca-leaching (Fig. 10). A similar assemblage of alteration types is observed in the area of the Central Duparquet mine, where silicification, carbonatisation, and K-feldspar alteration are less intense than in the Beattie mine area (Fig. 10). The significant assemblage of alteration types associated with the Beattie gold deposit is thus the following: carbonatisation, K-feldspar alteration, silicification, and Na-Ca-leaching.

Alteration mechanisms

The most characteristic and widespread alteration types associated with orogenic gold deposits are carbonatisation and alkali metasomatism, which usually form sericite and, less commonly, K-feldspar and albite (see Groves *et al.* 1998 and references therein). Hydration, sulfurization, and silicification are also common, and alteration minerals are generally dependant on the composition of the precursor (Groves *et al.* 1998). By comparison with an analogous alkaline intrusion such as Murdoch Creek (Rowins *et al.* 1991, 1993), it is proposed that the Beattie Syenite contained mostly alkali feldspar and

clinopyroxene prior to alteration. Carbonatisation and hydration of such rocks may potentially form carbonates, quartz, and minor amounts of chlorite and white mica, and leach substantial amounts of alkali (see Equation 3).

It is proposed that carbonatisation and hydration may be the leading processes that redistributed a large amount of SiO_2, Na_2O, K_2O, and CaO in the Beattie Syenite. According to this hypothesis, the K-feldspar alteration and Na-leaching are only intense because the precursor was enriched in alkali. This hypothesis does not exclude an external source for K_2O. However and with the available data, the amount of K_2O that the hydrothermal fluid may have added to the system cannot be distinguished from that locally re-distributed within the intrusion. A similar result applies to SiO_2. The intensity of K-feldspar alteration, silicification, and Na-Ca-leaching is thus particular to Beattie and strongly controlled by the alkaline nature of the precursor. The nature and composition of the hydrothermal fluid are likely similar to these generally reported for orogenic gold deposits (i.e. low-salinity H_2O-CO_2-CH_4-bearing fluids; e.g. Groves *et al.* 1998).

Alteration quantification and exploration

Many methods are available to quantify hydrothermal alteration types, but only a handful of these tools can be realistically applied in an exploration context, as is discussed here.

Carbonatisation, for instance, can be quantified using the proportion of carbonates observed in hand samples, which is generally unreliable, or counted in thin sections, which is expensive and time consuming. Alternatively, carbonatisation can be satisfactorily estimated from CO_2 wt%, which is also an expensive solution. For example, the package for whole rock analysis proposed by Actlabs Ltd. includes the LOI, but analysis of CO_2 wt% adds an extra cost of $18.50 per sample. Carbonatisation is thus best quantified from LOI, using either the NORMAT (Piché & Jébrak 2004) or the CONSONORM_LG (Trépanier *et al.* 2015) methods. These normative methods are particularly adapted to exploration purposes as they only require the analysis of major elements. The CONSONORM_LG method can also distinguish between the chlorite and white mica formed by chloritisation and sericitisation processes from these produced by carbonatisation, and provide satisfactory estimates of the intensity of sericitisation and chloritisation.

Like carbonatisation, silicification is relatively easy to estimate from thin sections or alteration indices because the precursor contained little to no quartz and carbonate. Indices are adapted to the quantification of gains but cannot easily be used to estimate leaching, which is best documented by mass-balance calculations.

Quantifying alkali metasomatism in an alkali-enriched intrusion is particularly challenging. Observed and normative minerals are of little help, as alteration intensity can only be deduced if the orthoclase and albite content of the precursor is known. The identification of a suitable precursor is possibly the most difficult step to any quantification of alteration. The studied intrusion was not homogeneous prior to

alteration and the available precursor applies only to Group I samples. This precursor was used to calculate the PER_K index. The advantage of such an index is that, even by arbitrarily selecting a value for the orthoclase/albite ratio of the precursor, the index still reaches values of 100 and -100 where K- and Na-gains, respectively, are maximal.

However, the PER diagrams method (Pearce 1968; Stanley & Madeisky 1994) is difficult to use because it requires the identification and analysis of conserved elements and detailed knowledge of the petrology of the examined rocks such as, in this case, of the nature of the minerals that control most of the Na_2O, K_2O, CaO, and Al_2O_3 distribution. Mass-balance calculations (e.g. Grant 1986; Barrett & MacLean 1994; Trépanier *et al.* 2016), on the other hand, require the sampling of a precursor and/or the analysis of trace elements. Despite the advantage of this method that precisely quantifies mass changes, its requirements may make it difficult to apply in an exploration context. In the studied area, the lack of systematic trace element analyses prevented the modelling of precursor compositions (Trépanier *et al.* 2016) and mass-balance calculations could only be performed on Group I samples and using the best precursor available.

In summary, alteration indices calculated using normative minerals are a powerful alternative to time-consuming detailed mineralogical observations. For alteration types that cannot be quantified using such indices, mass-balance calculations likely constitute the most powerful method, but must be applied with care and only once the amount of geological data available is sufficient to enable the sampling of a reliable precursor. Alternatively, systematic analyses of trace elements allow for the modelling of precursor compositions (see Trépanier *et al.* 2016). This method is particularly adapted to multi-precursor magmatic systems for which precursors cannot be easily sampled.

Conclusions

The Beattie gold mineralisation is hosted by a Neoarchean alkaline intrusion of the Abitibi Subprovince, Québec. Intense silicification, K-feldspar alteration, and Na-Ca-leaching are spatially correlated with gold occurrences, while carbonatisation is widespread and intense. Metasomatism is thus mostly characterised by Si-K-CO_2-gains and Na-Ca-losses in the mineralised area. Possibly, carbonatisation and hydration turned most clinopyroxenes and a portion of the feldspars into calcite, quartz, sericite, and chlorite, and triggered the re-distribution of alkali elements within the intrusion.

Using the chemical dataset compiled by Bourdeau (2013), carbonatisation and silicification are best quantified by normative minerals and related alteration indices from the CONSONORM_LG method (Trépanier *et al.* 2015), and good constraints on K-feldspar alteration are obtained using the PER diagram method (Pearce 1968; Stanley & Madeisky 1994). Mass-balance calculations, on the other hand, could not be applied on the whole dataset as trace elements analyses are scarce and the available precursor could only be used for a part of the samples. The mass-balance method does, however, provide results that are consistent with those obtained using other methods and is particularly adapted to the quantification of Na-Ca-leaching.

In an exploration context, obtaining reliable and abundant analyses of trace elements and sampling precursors in poorly documented areas can be problematic, and can prevent the calculation of mass changes. The PER diagram method can only be used in particular situations, where the precursors have a magmatic origin and if constraints on the fractional crystallisation process are available. Alteration indices, on the other hand, are useful if their values are close to zero in precursors, but cannot easily be used to quantify silicification, for example, if the precursor is a quartz-rich rock. The available methods thus have their particular advantages and disadvantages, which must be acknowledged so that alteration halos and hydrothermal processes can be properly delimited and understood.

Special thanks are addressed to Stephen Amor, to editor Kurt Kyser, and to an anonymous reviewer who greatly help to improve this contribution. This study was performed on behalf of the CONSOREM research group (Consortium de Recherche en Exploration Minérale). This project was supported by Canada Economic Development for Quebec Regions, the Ministère de l'Énergie et des Ressources Naturelles du Québec (MERN), the Conférence Régionale des Élus Saguenay-Lac-Saint-Jean (CRÉ), and companies members of CONSOREM. The author addresses warm thanks to her supervisor and colleagues, Réal Daigneault, Silvain Rafini, Stéphane Faure, and Ludovic Bigot for constructive comments. Special thanks are addressed to Sylvain Trépanier (Osisko Gold Royalties Ltd.) and Jean Goutier (MERN), for our many discussions. The author is indebted to the members of CONSOREM for defining this project and for stimulating discussions on this topic throughout 2014 and 2015.

References

Banfield, A.F. 1940. *The Geology of Beattie Gold Mines (Québec) Limited, Duparquet, Québec, Canada.* PhD thesis, Northwestern University, Evanston, United States.

Barrett, T.J., & MacLean, W.H. 1994. Chemostratigraphy and hydrothermal alteration in exploration for VHMS deposits in greenstones and younger volcanic rocks. *In:* Lentz, D.R. (ed) *Alteration and alteration processes associated with ore-forming systems.* Geological Association of Canada, Short Course Notes **11**, 433-467.

Beakhouse, G.P. 2011. *The Abitibi Subprovince plutonic record: Tectonic and metallogenic implications*. Ontario Geological Survey, Open File Report, **OF-6268**.

Bigot, L. 2012. *Gold mineralizations at the syenite-hosted Beattie gold deposit at Duparquet, neoarchean Abitibi belt, Québec, Canada*. Master's thesis, Université du Québec à Montréal (UQAM), Montréal, Canada.

Bigot, L., & Jébrak, M. 2015. Gold Mineralization at the Syenite-Hosted Beattie Gold Deposit, Duparquet, Neoarchean Abitibi Belt, Canada. *Economic Geology,* http://doi.org/10.2113/econgeo.110.2.315

Bourdeau, J. 2013. *Petrology, Mineralogy and Geochemistry of the Beattie Syenite and Country Rocks, Abitibi Greenstone Belt, Québec.* Master's thesis, Ottawa University, Ottawa, Canada.

Bourne, J.H., & L'Heureux, M. 1991. The petrography and geochemistry of the Clericy Pluton: an ultrapotassic pyroxenite-syenite suite of late Archaean age from the Abitibi region, Quebec. *Precambrian Research*, http://doi.org/10.1016/0301-9268(91)90012-Y

David, J., Davis, D.W., Dion, C., Goutier, J., Legault, M., & Roy, P. 2007. *Datations U-Pb effectuées dans la Sous-province de l'Abitibi en 2005-2006.* Ministère des Ressources naturelles et de la Faune (Québec) Report, **RP-2007-01**.

Davidson, S.C., & Banfield, A.F. 1944. Geology of the Beattie gold mine, Duparquet, Quebec. *Economic Geology*, **39**, 535-556.

Dejou, B. 1992. *Étude pétrographique et géochimique de la syénite du lac Tarsac, canton Montbray, Abitibi, Québec / Petrographic and chemical study of the Tarsca syenite, Montbray area, Abitibi, Montréal, Canada.* Master's thesis, École polytechnique, Québec.

Grant, J.A. 1986. The isocon diagram - a simple solution to Gresen's equation for metasomatic alteration. *Economic Geology,* http://doi.org/10.2113/gsecongeo.81.8.1976

Grant, J.A. 2005. Isocon analysis: a brief review of the method and applications. *Physics and Chemistry of the Earth,* Parts A/B/C, **30**, 997-1004.

Gresens, R.L. 1967. Composition-volume relationships in metasomatism. *Chemical Geology*, http://doi.org/10.1016/0009-2541(67)90004-6

Groves, D.I., Goldfarb, R.J., Gebre-Mariam, M., Hagemann, S.G., & Robert, F. 1998. Orogenic gold deposits: a proposed classification in the context of their crustal distribution and relationship to other gold deposit types. *Ore geology reviews*, http://doi.org/10.1016/S0169-1368(97)00012-7

Hofmann, A.W. 1988. Chemical differentiation of the Earth: the relationship between mantle, continental crust, and oceanic crust. *Earth and Planetary Science Letters*, **90**, 297-314.

Kishida, A., & Kerrich, R.D. 1987. Hydrothermal alteration zoning and gold concentration at the Kerr-Addison lode gold deposit, Kirkland Lake, Ontario. *Economic Geology*, http://doi.org/10.2113/gsecongeo.82.3.649

Large, R.R., Gemmell, J.B., Paulick, H., & Huston, D.L. 2001. The alteration box plot: A simple approach to understanding the relationship between alteration mineralogy and lithogeochemistry associated with volcanic-hosted massive sulfide deposits. *Economic Geology*, http://doi.org/10.2113/gsecongeo.96.5.957

593 Legault, M., & Lalonde, A.E. 2009. Discrimination des syénites associées aux gisements
594 aurifères de la sous-province de l'Abitibi, Québec, Canada. Ministère des Ressources
595 naturelles et de la Faune (Québec) Report, **RP 2009-04**.
596
597 Legault, M., Goutier, J., Beaudoin, G., & Aucoin, M. 2006. Metallogenic synthesis of the
598 Porcupine-Destor Fault, Abitibi Subprovince. Ministère des Ressources naturelles et de la
599 Faune (Québec) Report, **ET-2006-01.**
600
601 Leitch, C.H.B., & Lentz, D.R. 1994. The Gresens approach to mass balance constraints of
602 alteration systems: methods, pitfalls, examples. *In:* Lentz, D.R. (ed) *Alteration and*
603 *alteration processes associated with ore-forming systems.* Geological Association of
604 Canada, Short Course Notes **11**, 161-192.
605
606 MacLean, W.H., & Barrett, T.J. 1993. Lithogeochemical techniques using immobile
607 elements. *Journal of geochemical exploration*, **48**, 109-133.
608
609 Mathieu, L., Trépanier, S., & Daigneault, R. 2015. CONSONORM_HG: a new method of
610 norm calculation for mid-to high-grade metamorphic rocks. *Journal of Metamorphic*
611 *Geology*, http://doi.org/10.1111/jmg.12168
612
613 Martin, R.D. 2012. *Syenite-hosted gold mineralization and hydrothermal alteration at the*
614 *Young-Davidson deposit, Matachewan,* Ontario. Master's Thesis, Waterloo University,
615 Waterloo, Canada.
616
617 McNicoll, V., Goutier, J., Dubé, B., Mercier-Langevin, P., Ross, P.S., Dion, C.,
618 Monecke, T., Legault, M., Percival, J., & Gibson, H. 2014. U-Pb Geochronology of the
619 Blake River Group, Abitibi Greenstone Belt, Quebec, and Implications for Base Metal
620 Exploration. *Economic Geology,* http://doi.org/10.2113/econgeo.109.1.27
621
622 Middlemost, E.A. 1989. Iron oxidation ratios, norms and the classification of volcanic
623 rocks. *Chemical Geology*, **77,** 19-26.
624
625 Mueller, W., Mortensen, J.K., Daigneault, R., & Chown, E.H. 1996. Archean terrane
626 docking: upper crust collision tectonics, Abitibi greenstone belt, Quebec, Canada.
627 *Tectonophysics,* http://doi.org/10.1016/S0040-1951(96)00149-7
628
629 Pearce, T.H. 1968. A contribution to the theory of variation diagrams. *Contributions to*
630 *Mineralogy and Petrology*, http://doi.org/10.1007/BF00635485
631
632 Pearce, J.A. 2008. Geochemical fingerprinting of oceanic basalts with applications to
633 ophiolite classification and the search for Archean oceanic crust. *Lithosphere*, **100**, 14-48.
634
635 Pearson, V., & Daigneault, R. 2009. An Archean megacaldera complex: the Blake River
636 Group, Abitibi greenstone belt. *Precambrian Research,* **168**, 66-82.
637

638 Piché, M., & Jébrak, M. 2004. Normative minerals and alteration indices developed for
639 mineral exploration. *Journal of Geochemical Exploration*,
640 http://doi.org/10.1016/j.gexplo.2003.10.001
641
642 Powell, W.G., Carmichael, D.M., & Hodgson, C.J. 1995. Conditions and timing of
643 metamorphism in the southern Abitibi greenstone belt, Québec. *Canadian Journal of*
644 *Earth Sciences,* http://doi.org/10.1139/e95-067
645
646 Rowins, S.M., Cameron, E.M., Lalonde, A.E., & Ernst, R.E. 1993. Petrogenesis of the
647 late Archean syenitic Murdock Creek pluton, Kirkland Lake, Ontario: evidence for an
648 extensional tectonic setting. *Canadian Mineralogist,* **31**, 219-230.
649
650 Rowins, S.M., Lalonde, A.E., & Cameron, E.M. 1991. Magmatic oxidation in the syenitic
651 Murdock Creek intrusion, Kirkland Lake, Ontario: evidence from the ferromagnesian
652 silicates. *The Journal of Geology,* **99**, 395-414.
653
654 Saeki, Y., & Date, J. 1980. Computer application to the alteration data of the footwall
655 dacite lava at the Ezuri Kuroko deposits, Akito Prefecture. *Mining Geology,* **30**, 241-250.
656
657 Shand, S.J. 1927. On the relations between silica, alumina, and the bases in eruptive
658 rocks, considered as a means of classification. *Geological Magazine,* **64**, 446-449.
659
660 Shand, S.J. 1951. *Eruptive rocks.* John Wiley and Sons, New York.
661
662 Stanley, C.R., & Madeisky, H.E. 1994. Lithogeochemical exploration for hydrothermal
663 ore deposits using Pearce element ratio analysis: Alteration and alteration processes
664 associated with ore forming systems. *In:* Lentz, D.R. (ed) *Alteration and alteration*
665 *processes associated with ore-forming systems.* Geological Association of Canada, Short
666 Course Notes **11**, 193-211.
667
668 Trépanier, S., Mathieu, L., & Daigneault, R. 2015. CONSONORM_LG: new normative
669 minerals and alteration indices for low-grade metamorphic rocks. *Economic*
670 *Geology*, **110**, 2127-2138.
671
672 Trépanier, S., Mathieu, L., Daigneault, R., & Faure, S. 2016. Precursors predicted by
673 artificial neural networks for mass balance calculations: Quantifying hydrothermal
674 alteration in volcanic rocks. *Computers & Geosciences*,
675 http://doi.org/10.1016/j.cageo.2016.01.003
676

Figure captions

Fig. 1. Maps of the Beattie Syenite adapted from Bourdeau (2013) and displaying local geology (**a**) and mineralisation (**b**). The geographic projection is UTM (NAD83, zone 17U).

Fig. 2. Primitive mantle-normalised spider-diagram displaying 32 Beattie Syenite samples for which trace elements are available. Primitive mantle composition is from Hofmann (1988) and element order is from Pearce (2008).

Fig. 3. TiO_2 vs Al_2O_3 binary diagrams displaying: (**a**) samples form the Murdock Creek alkaline intrusion collected and described by Rowins *et al.* (1993); (**b**) the Beattie Syenite samples classified using lithological units defined by Bourdeau (2013). The Murdock Creek intrusion has not been altered (Rowins *et al.* 1991) and its samples define a fractionation trend. The samples from the Beattie Syenite define two main alteration trends (as defined by Barrett & MacLean 1994) and are thus distributed between Groups I and II. An hypothetical fractionation trend, for the Beattie Syenite, is also represented.

Fig. 4. Box plot diagrams displaying the results of mass-balance calculations for Group I samples (see Fig. 3-b).

Fig. 5. K_2O vs Na_2O displaying the results of mass-balance calculations for Group I samples (see Fig. 3). Note that K- and Na-gains are negatively correlated, and that maximal total mass gains correlate with maximal K-gains.

Fig. 6. Box plot diagrams displaying the normative compositions of the Beattie Syenite samples (**a**) and the values of the alteration indices (**b**) calculated with the CONSONORM_LG method. The "%Or" factor is equivalent to the orthoclase/albite ratio and is calculated as follows: 100*orthoclase/(orthoclase+albite).

Fig. 7. PER diagrams for feldspar (**a**, **b**), alkali feldspar (**c**), and orthoclase (**d**). Feldspar is not the only phase that may contain Ca, which is also found within the alteration mineral calcite and was likely accommodated by clinopyroxene prior to alteration. To take these mineralogical constraints into account, Mg (**a**) or C (**b**) is subtracted from Ca. The samples of Group I, II, and III, as defined from the TiO_2 vs Al_2O_3 binary diagram (Fig. 3-b), are also identified (**d**).

Fig. 8. Binary diagrams displaying correlations between alteration types quantified with various methods: (**a**) PER_K index vs K_2O mass change; (**b**) ALT_QTZ index vs SiO_2 mass change (one sample, for which a SiO_2 mass change of 831% has been calculated and that likely contains a quartz-vein is not represented). The coefficients of determination are calculated for polynomial (2^{nd} order) regression lines.

Fig. 9. Maps of the Beattie Syenite intrusion, as outlined by Bourdeau (2013), displaying the values of the PER_K index (**a**), the ALT_CARBS index (**b**), the ALT_QTZ index (**c**), the CaO and Na_2O mass changes (**d**); and the gold values (**e**). The spatial interpolation is inverse distance squared (ID2) and its results are colour coded using equal intervals (**a, b, c, d**).

Fig. 10. Simplified map of the dominant alteration types documented in the Beattie Syenite intrusion, as outlined by Bourdeau (2013). Alteration types were interpolated using ID2 (see Fig. 9).

Table 1. *Source of the chemical data compiled by Bourdeau (2013)*

	Samples with analysed:		
Source	**Major elements**	**Y, Zr, Nb, Th, Cr**	**Analytical method**
Banfield, 1940	14	0	unavailable
Gold Fields Resources Canada Ltd., 1981	6	6 (Cr, Zr)	XRF
MRNF, 1990 to 2010	38	38	XRF, ICP-AES, ICP-MS
Noranda Exploration Ltd., 1991	1	0	XRF
Osisko Mining Corporation, 2010	86	7 (Cr)	ICP-AES
SOQUEM, 1980	40	1	AAS, XRF
TOTAL	**185 samples**		

735

736 **Table 2.** *Precursor composition (average of 5 samples; from Bigot & Jébrak 2015)*

	Avg.	Std. dev.
SiO_2 (wt%)	57.76	*1.32*
TiO_2	0.57	*0.02*
Al_2O_3	16.4	*1.2*
$Fe_2O_3^T$	5.22	*0.3*
MnO	0.11	*0.03*
MgO	1.4	*0.52*
CaO	3.8	*1.45*
Na_2O	5.47	*0.17*
K_2O	4.55	*0.66*
P_2O_5	0.32	*0.07*
C	0.94	*0.48*
S	0.04	*0.01*
LOI	2.99	*1.62*
TOTAL	98.4	*0.91*
Cr (ppm)	10	*0*
Nb	12.45	*0.53*
Th	25.15	*2.07*
Y	34.55	*3*
Zr	356.75	*29.61*

737
738
739

740

741 **Table 3.** *Alteration indices of the CONSONORM_LG method*

Indices	Formula
ALT_CHLO	100 × (chlorite_Mg × 0.75 + chlorite_Fe) / SUM01*
ALT_MUSCV	100 × muscovite / SUM01*
ALT_QZT†	100 × quartz / SUM02‡
ALT_ALB†	100 × albite / SUM02‡
ALT_KFS†	100 × orthoclase / SUM02‡
ALT_SER_CARBS	100 × (ankerite + dolomite + magnesite + siderite + muscovite – muscovite_WITHOUTCO2) / (SUM03§ + orthoclase + muscovite)
ALT_CARB¶	100 × (calcite + dolomite + ankerite + magnesite + siderite) / SUM03§

742

743 *SUM01 = sum of all minerals (with chlorite_Mg multiplied by 0.75), except quartz and
744 sulfides.
745 †These indices are not part of the CONSONORM_LG method and have been formulated
746 to meet the need of this study.
747 ‡SUM02 = sum of all silicates, quartz included (with chlorite_Mg multiplied by 0.75).
748 §SUM03 = sum of all FeO-, MgO- or/and CaO-bearing minerals, except sulfides.
749 ¶ALT_CARBS: similar to the IPAF index of NORMAT (Piché & Jébrak 2004).
750
751
752

753

754

Table 4. *Normative minerals and alteration indices (median values) calculated with the CONSONORM_LG method*

	Precursor* (n= 1)	Equigranular magnetite-bearing syenite (n= 3)	Mega--porphyritic syenite (n= 7)	Porphyritic Beattie syenite (n= 131)	Central Duparquet syenite (n= 33)	Lath syenite (n= 4)
Albite (wt%)	46.92	46.06	36.31	33.35	37.15	34.78
Orthoclase†	27.26	29.45	31.28	27.54	26.38	32.5
Muscovite†	0	0	8.43	7.83	10.01	7.63
Quartz	3.95	2.78	12.7	12.06	9.91	2.04
Chlorite	6.46	5.11	1.75	0.82	0.66	2.29
Epidote	3.94	4.55	0.11	0.11	0.11	3.48
Carbonate	3.42	0.93	1.11	6.49	6.42	2.49
Oxyde Fe-Ti	2.22	2.12	2.67	2.25	2.01	2.29
Sulphide	1.84	0.11	0.42	0.27	0.16	0.26
Other‡	4	8.86	1.28	0.92	0.93	3.36
ALT_CHLO	0.62	3.74	2.15	0.39	1.6	4.34
ALT_MUSCV	0	0	0	0	0	0
ALT_QTZ	4.31	2.88	14.08	13.5	11.26	2.19
ALT_ALB	50.23	47.81	36.53	38.15	42.54	37.18
ALT_KFS	29.19	30.51	39.63	31.81	33.37	33.39
ALT_SER_CARBS	0	0	5.16	19.84	28.04	9.59
ALT_CARBS	21.01	4.41	66.69	72.8	83.1	15.78

*Precursor: average of 5 samples (from Bigot & Jébrak 2015)

†The normative K-feldspar is named orthoclase. Distinction between microcline, andaluria, and orthoclase is not attempted by the normative calculation. Idem for white mica (i.e. muscovite-paragonite vs sericite).

‡Other minerals: paragonite, talc, grunerite, tremolite, ferroactinolite, apatite, chromite, titanite, rutile, halite, sylvite, and anhydrite.

Table 5. *Alteration intensity compared to the gold content of samples*

Au (ppm)	**5000-20000**	**1000-5000**	**100-1000**	**0-100**
Masse change (%)				
n*	7	26	16	69
SiO_2†	40.63	19.64	3.31	-0.29
FeO^T	0.97	-0.11	-0.06	-0.78
CaO	-1.78	-2.25	-1.19	-0.36
MgO	-0.71	-1.04	-0.54	-0.65
Na_2O	-5.29	-5.06	-4.25	-0.55
K_2O	7.00	7.79	4.91	0.48
Indices (dimensionless)				
n	11	32	18	91
ALT_CHLO†	1.49	0.41	1.73	1.64
ALT_SER	3.57	0	0	0
ALT_QZT	32.69	25.42	14.16	11.92
ALT_CHLO_CC_TLC	0	0	1.77	18.49
ALT_SER_CARBS	6.17	5.20	21.75	36.11
ALT_CARBS	84.42	92.06	93.13	73.56
PER_K	97.99	95.89	83.19	10.30

*Calculations are performed only on the 151 samples for which gold has been analysed.
†Median values are provided for each parameter.

Table 6. *Methods used to quantify alteration and their relevant values*

Method	Median	Threshold values*
K_2O mass change	1.62%	> 2%, significant K-gain
PER_K index	47.15	> 50, K-feldspar alteration
ALT_KFS index	32.42	> 38, K-feldspar alteration
Normative orthoclase	27.67 wt%	> 20 wt%, K-feldspar alteration
ALT_SER	0	?
Normative muscovite	8.70 wt%	?
Na_2O mass change	-1.54%	< -1.42%, Na-leaching
ALT_ALB index	39.51	< 42, Na-leaching
Normative albite	34.10 wt%	< 40 wt%, Na-leaching
ALT_CARBS index	72.81	> 70, intense carbonatisation
Normative carbonate	5.90 wt%	> 6 wt%, intense carbonatisation
Normative estimate of CO_2	2.63 wt%	> 2.6 wt%, intense carbonatisation
SiO_2 mass change	1.41%	> 25%, significant silicification
ALT_QTZ index	13	> 25, significant silicification
Normative quartz	11.24 wt%	> 22 wt%, significant silicification
CaO+Na_2O mass changes	-2.45%	< -2%, Ca-Na-leaching
FeO^T mass change	-0.52%	< -1%, Fe-leaching
MgO mass change	-0.65%	< -1%, Mg-leaching
ALT_CHLO	0.85	> 25, significant chloritisation

*Above or below the threshold value, the intensity of alteration is interpreted to be significant.

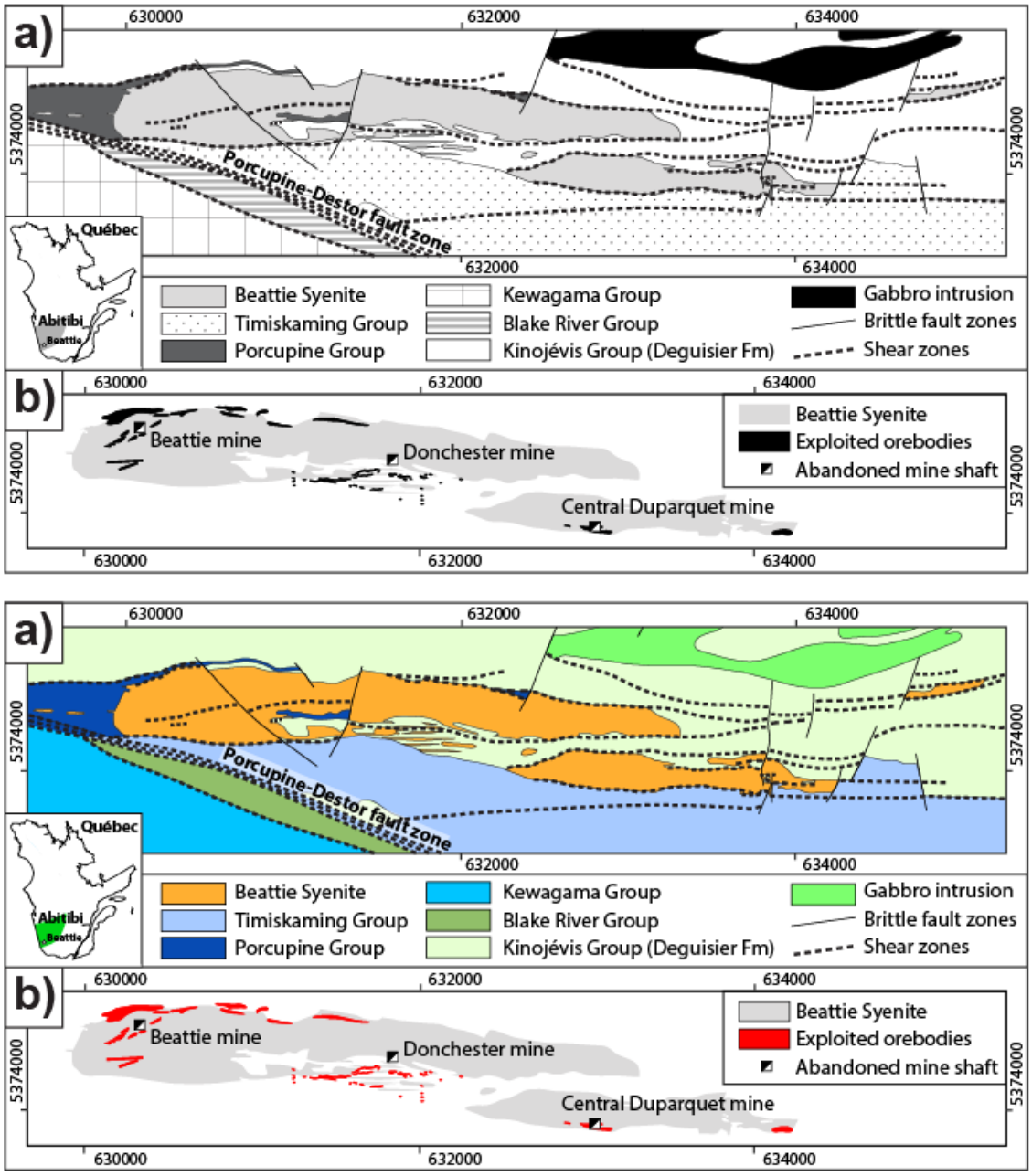
a)
630000
632000
634000
5374000
Porcupine-Destor fault zone
Québec
Abitibi
Beattie
Beattie Syenite
Timiskaming Group
Porcupine Group
Kewagama Group
Blake River Group
Kinojévis Group (Deguisier Fm)
Gabbro intrusion
Brittle fault zones
Shear zones
b)
Beattie mine
Donchester mine
Central Duparquet mine
Exploited orebodies
Abandoned mine shaft

Fig. 1

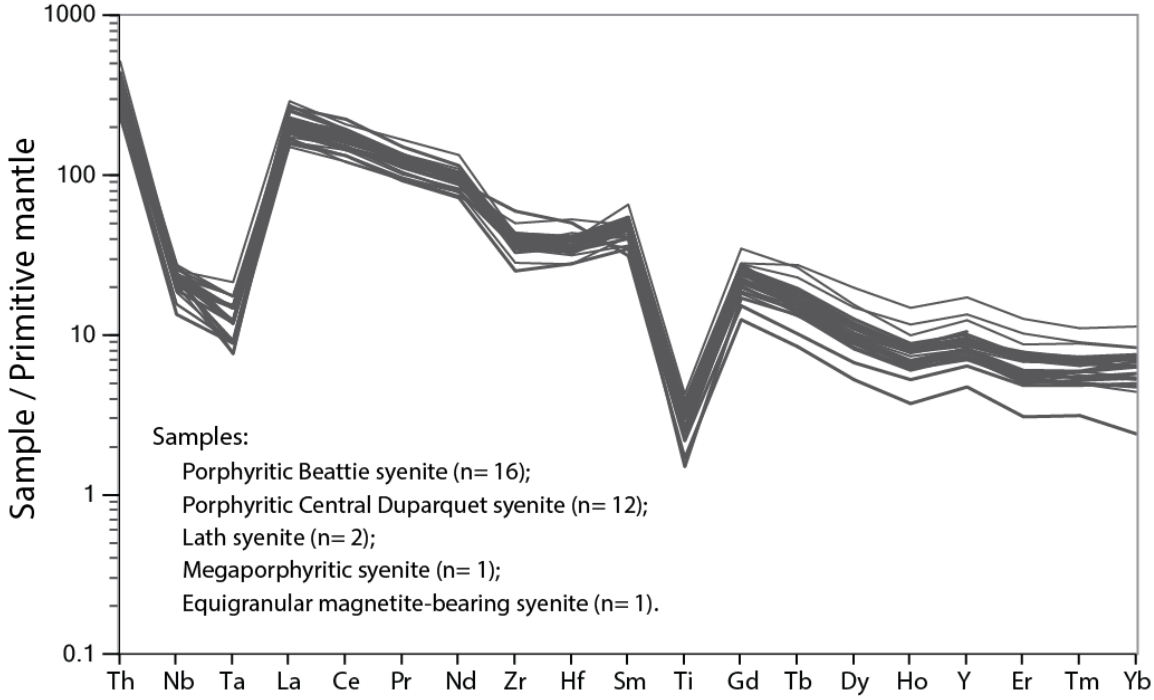
1000
100
10
1
0.1
Sample / Primitive mantle
Samples:
Porphyritic Beattie syenite (n= 16);
Porphyritic Central Duparquet syenite (n= 12);
Lath syenite (n= 2);
Megaporphyritic syenite (n= 1);
Equigranular magnetite-bearing syenite (n= 1).
Th Nb Ta La Ce Pr Nd Zr Hf Sm Ti Gd Tb Dy Ho Y Er Tm Yb

Fig. 2

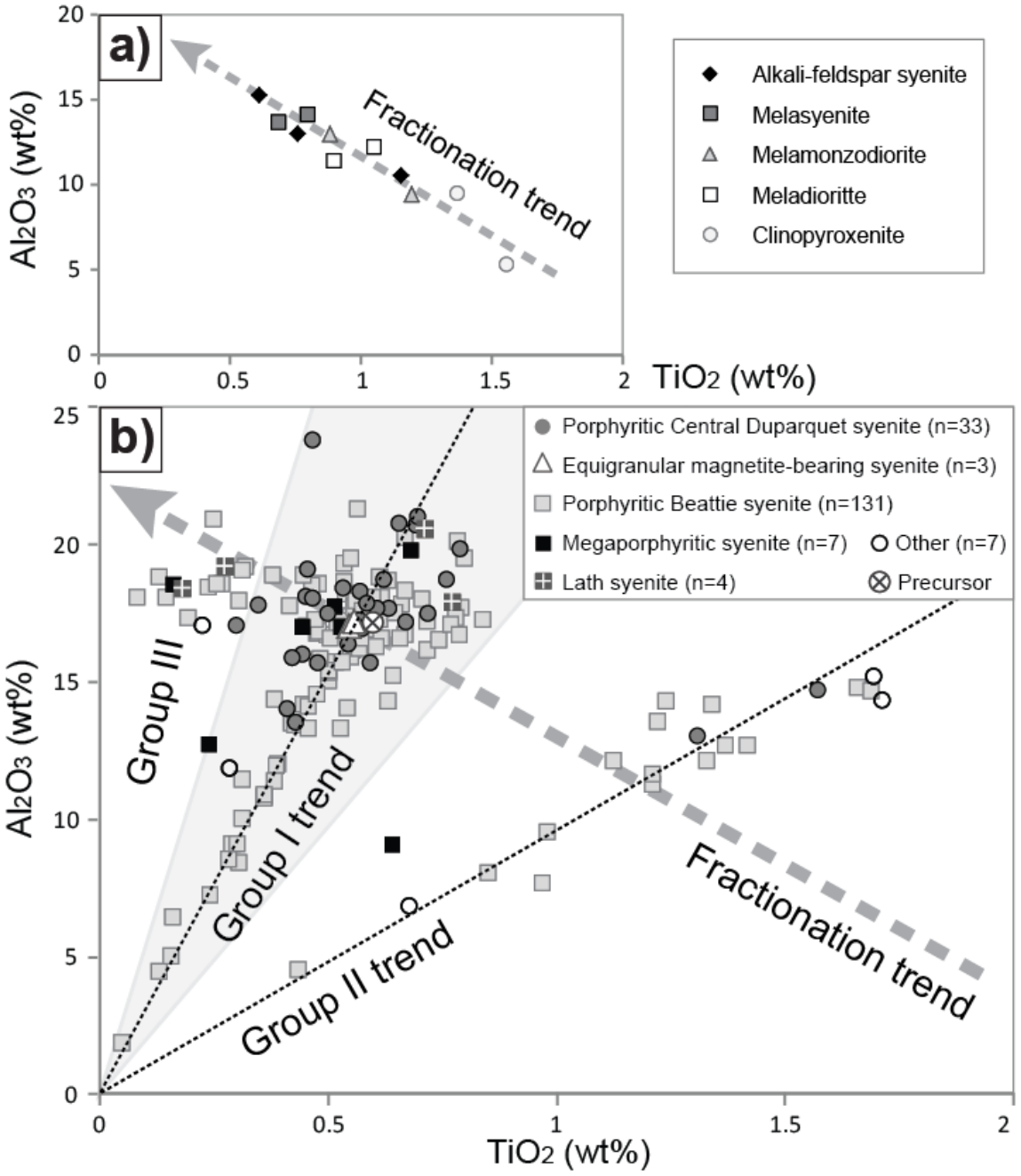

Fig. 3. TiO_2 vs Al_2O_3 binary diagrams displaying: (**a**) samples form the syenitic un-altered Murdock Creek intrusion, which have been collected and described by Rowins et al. (1993); (**b**) the Beattie Syenite samples classified using lithological units defined by Bourdeau (2013). The Murdock Creek intrusion has not been altered (Rowins et al. 1991) and its samples define a fractionation trend. The samples from the Beattie Syenite define two main alteration trends (as defined by Barrett and MacLean 1994) and are thus distributed between Group I and II. An hypothetical fractionation trend, for the Beattie Syenite, is also represented.

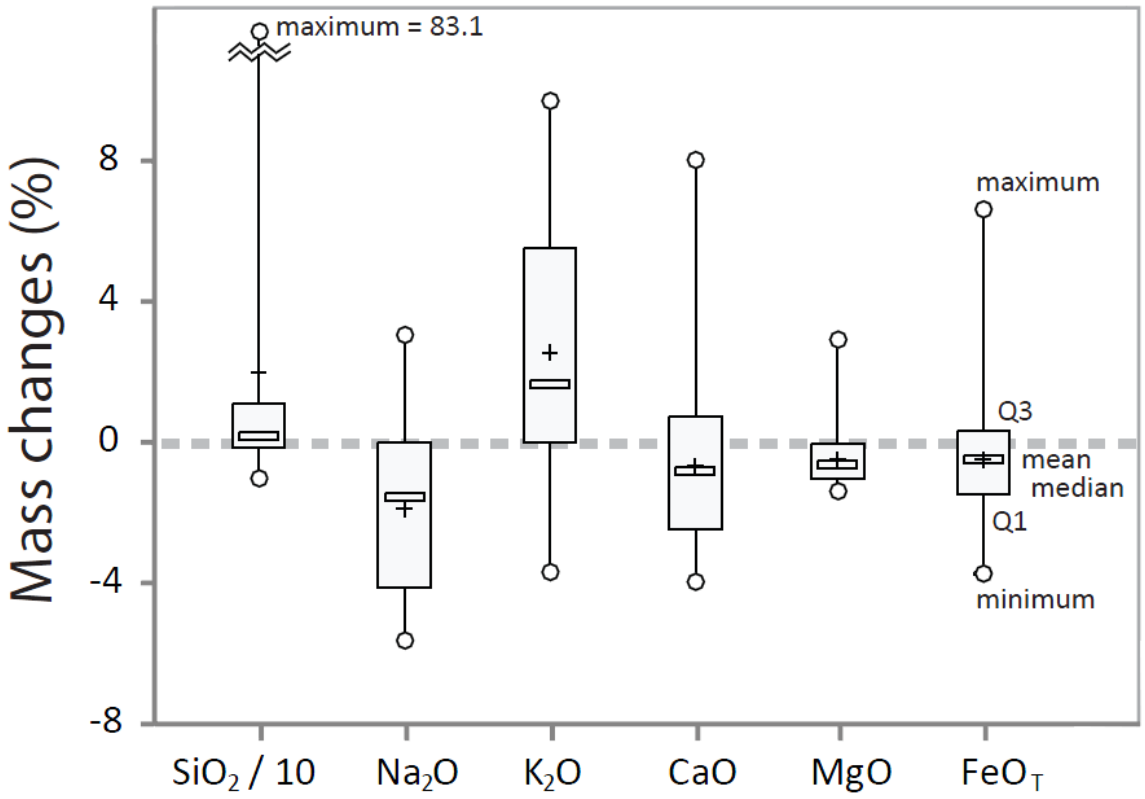
maximum = 83.1
Mass changes (%)
8
4
0
-4
-8
maximum
Q3
mean
median
Q1
minimum
SiO2 / 10
Na2O
K2O
CaO
MgO
FeOT

Fig. 4

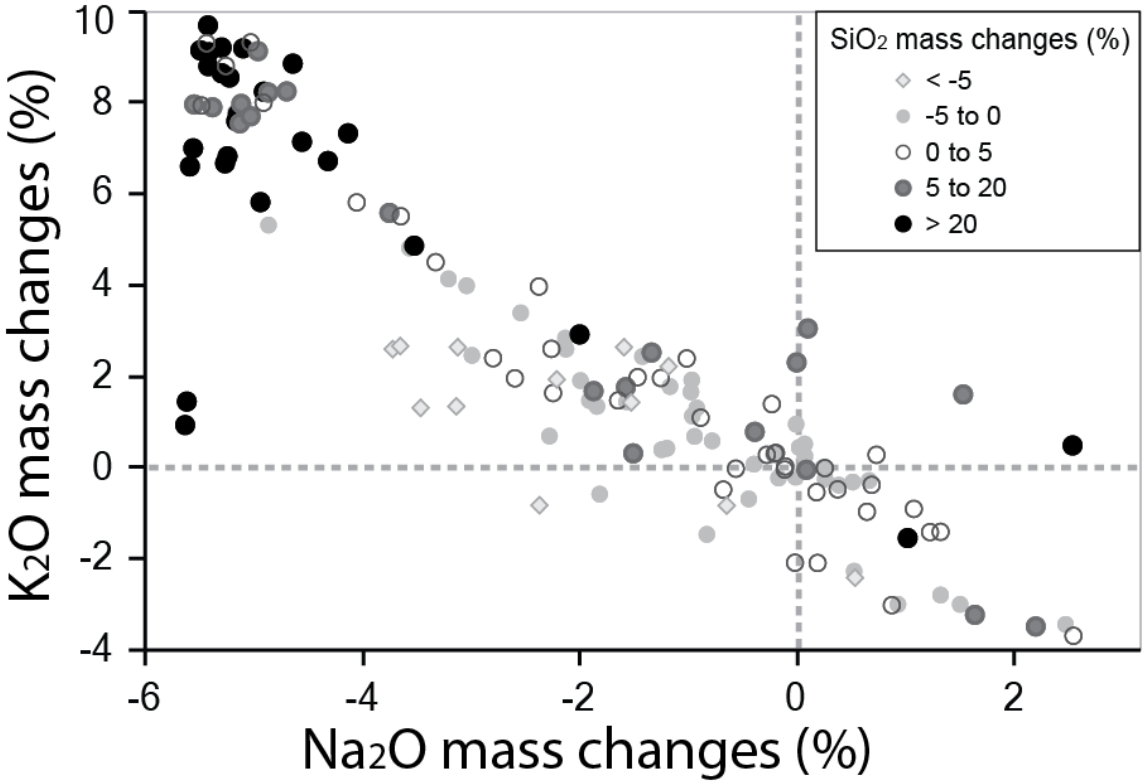
SiO2 mass changes (%)
< -5
-5 to 0
0 to 5
5 to 20
> 20
K2O mass changes (%)
Na2O mass changes (%)
10
8
6
4
2
0
-2
-4
-6
-4
-2
0
2

Fig. 5

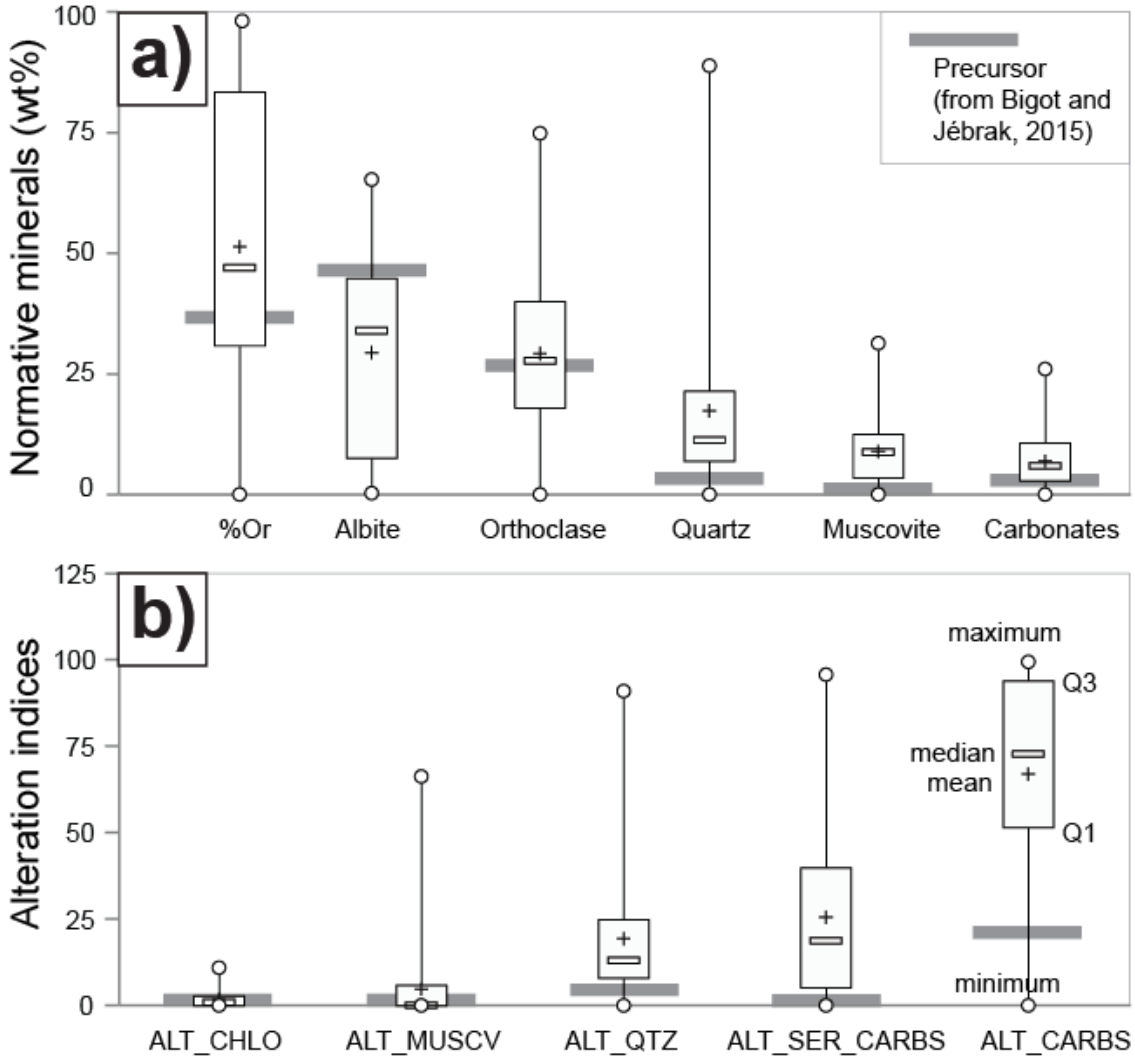
a)
Normative minerals (wt%)
100
75
50
25
0
Precursor
(from Bigot and
Jébrak, 2015)
%Or
Albite
Orthoclase
Quartz
Muscovite
Carbonates
b)
Alteration indices
125
100
75
50
25
0
maximum
Q3
median
mean
Q1
minimum
ALT_CHLO
ALT_MUSCV
ALT_QTZ
ALT_SER_CARBS
ALT_CARBS

Fig. 6

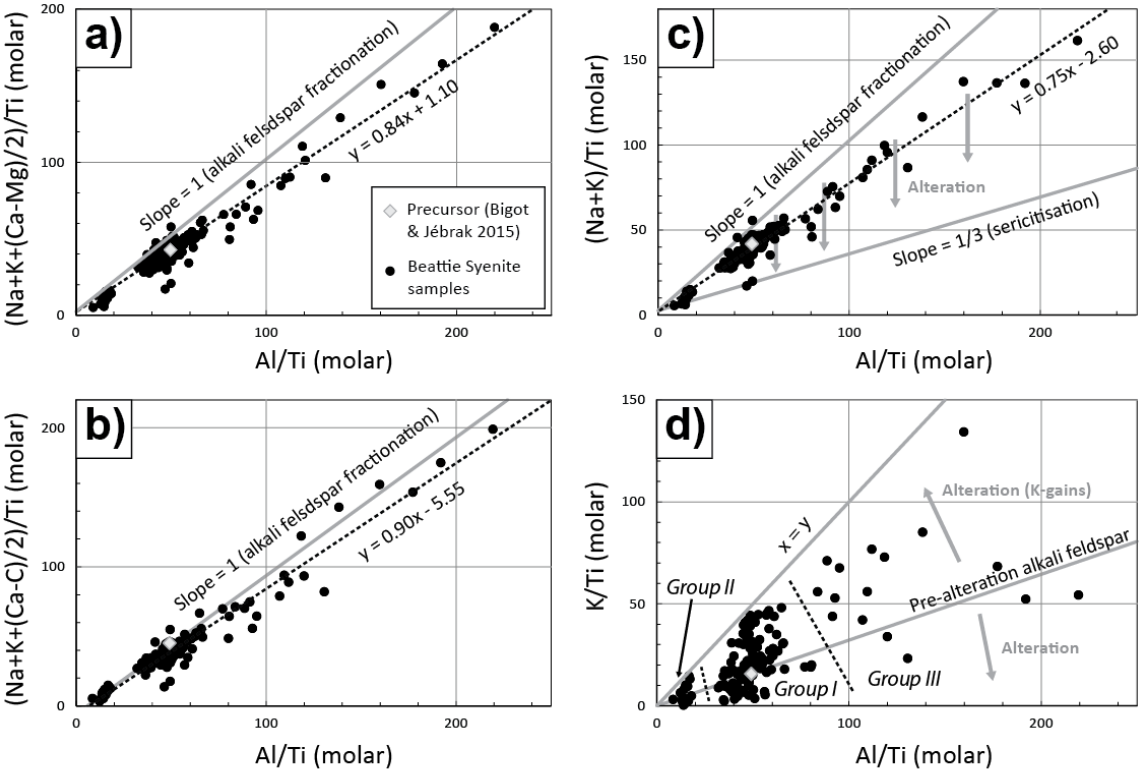
a)
(Na+K+(Ca-Mg)/2)/Ti (molar)
Al/Ti (molar)
Slope = 1 (alkali felsdspar fractionation)
y = 0.84x + 1.10
Precursor (Bigot & Jébrak 2015)
Beattie Syenite samples
b)
(Na+K+(Ca-C)/2)/Ti (molar)
Al/Ti (molar)
Slope = 1 (alkali felsdspar fractionation)
y = 0.90x - 5.55
c)
(Na+K)/Ti (molar)
Al/Ti (molar)
Slope = 1 (alkali felsdspar fractionation)
y = 0.75x - 2.60
Alteration
Slope = 1/3 (sericitisation)
d)
K/Ti (molar)
Al/Ti (molar)
Alteration (K-gains)
x = y
Group II
Pre-alteration alkali feldspar
Alteration
Group III
Group I

Fig. 7

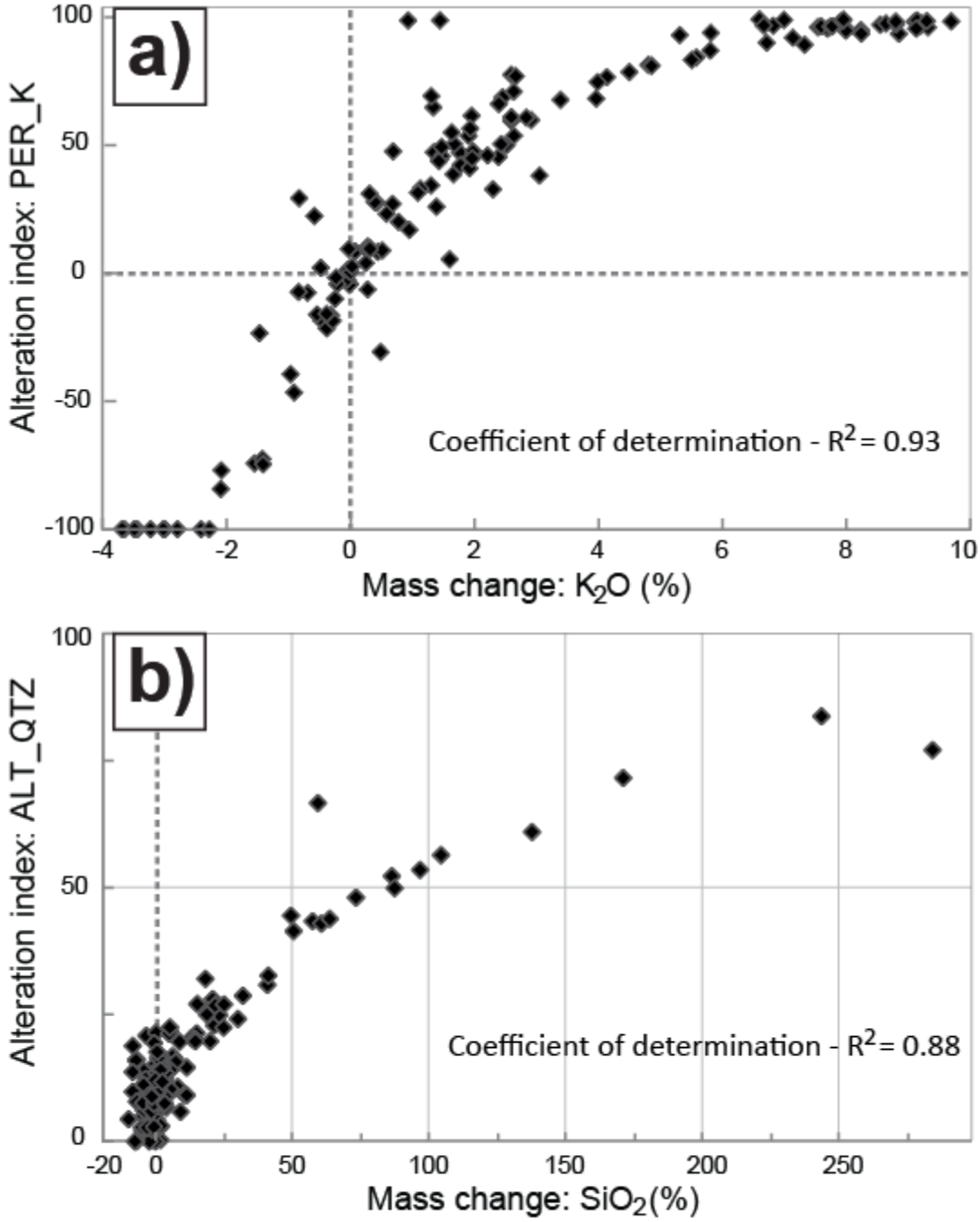
a)
Alteration index: PER_K
100
50
0
-50
-100
-4
-2
0
2
4
6
8
10
Mass change: K_2O (%)
Coefficient of determination - R^2 = 0.93
b)
Alteration index: ALT_QTZ
100
50
0
-20
0
50
100
150
200
250
Mass change: SiO_2(%)
Coefficient of determination - R^2 = 0.88

Fig. 8

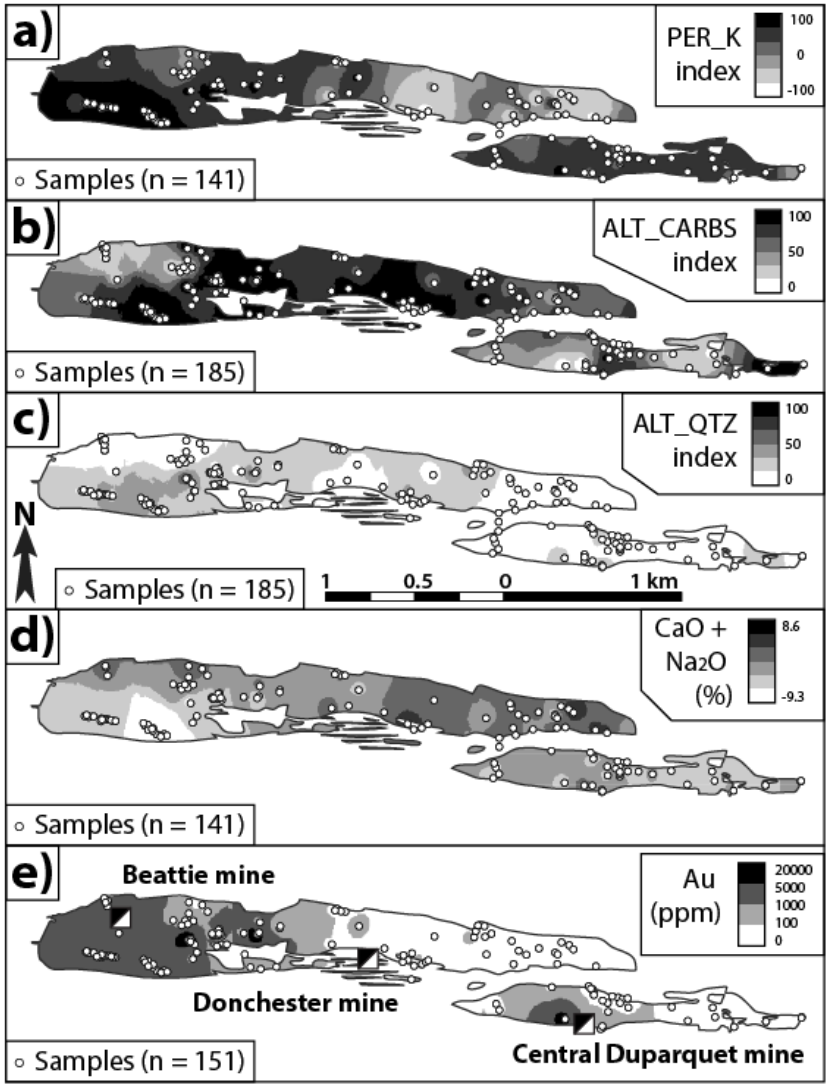
a)
PER_K index
100
0
-100
Samples (n = 141)
b)
ALT_CARBS index
100
50
0
Samples (n = 185)
c)
ALT_QTZ index
100
50
0
N
Samples (n = 185)
1 0.5 0 1 km
d)
CaO + Na2O (%)
8.6
-9.3
Samples (n = 141)
e)
Beattie mine
Au (ppm)
20000
5000
1000
100
0
Donchester mine
Central Duparquet mine
Samples (n = 151)

Fig. 09

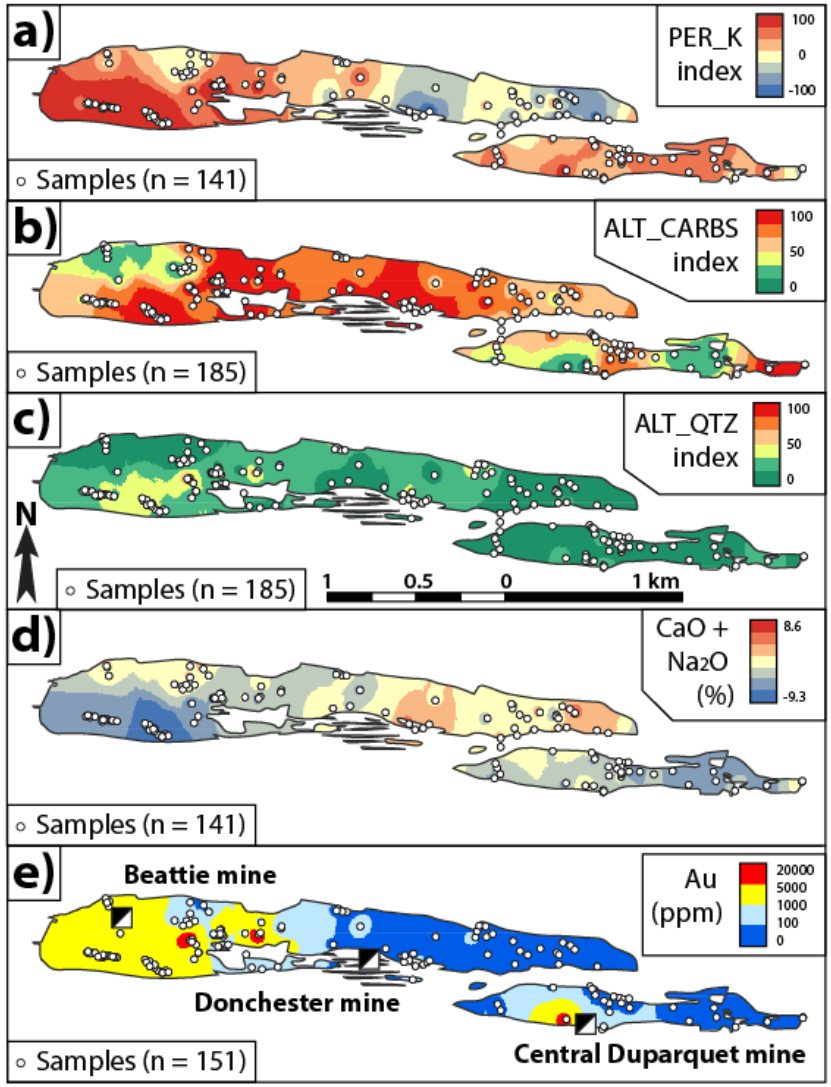
a)
PER_K index
100
0
-100
Samples (n = 141)
b)
ALT_CARBS index
100
50
0
Samples (n = 185)
c)
ALT_QTZ index
100
50
0
N
Samples (n = 185)
1 0.5 0 1 km
d)
CaO + Na2O (%)
8.6
-9.3
Samples (n = 141)
e)
Beattie mine
Au (ppm)
20000
5000
1000
100
0
Donchester mine
Central Duparquet mine
Samples (n = 151)

Fig. 09

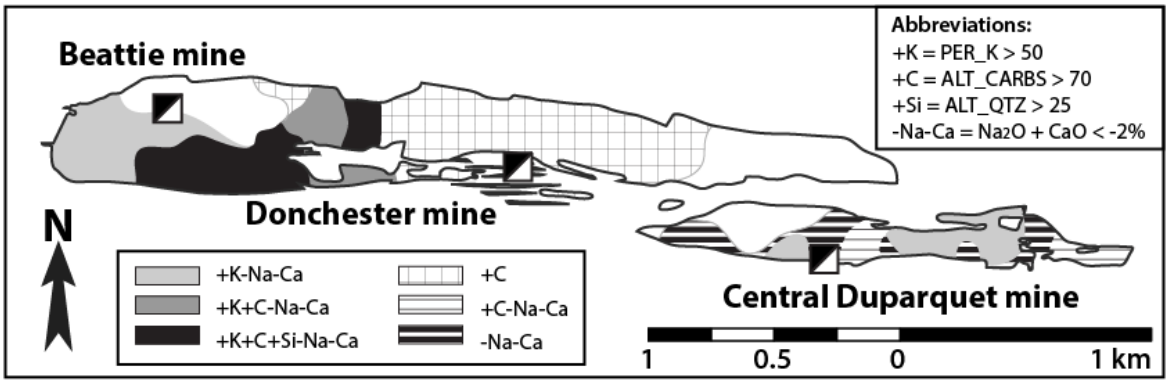

Fig. 10

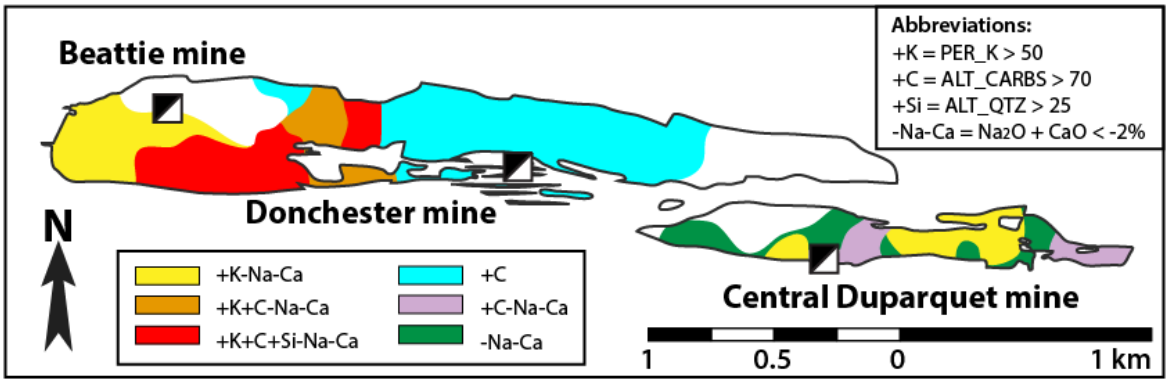

Fig. 10

1

2